

1 **Assessment of permafrost distribution maps in the Hindu** 2 **Kush Himalayan region using rock glaciers mapped in** 3 **Google Earth**

4 M. -O. Schmid¹, P. Baral¹, S. Gruber², S. Shahi¹, T. Shrestha¹, D. Stumm¹ and P. Wester^{1,3}

5 [1]{ICIMOD, International Centre for Integrated Mountain Development, GPO Box 3226,
6 Kathmandu, Nepal}

7 [2]{Department of Geography & Environmental Studies, Carleton University, Ottawa,
8 Canada}

9 [3]{Water Resources Management group, Wageningen University, Wageningen, the
10 Netherlands}

11 Correspondence to: M. -O. Schmid (marcolivier.schmid@gmail.com)

12 **Abstract**

13 The extent and distribution of permafrost in the mountainous parts of the Hindu Kush
14 Himalayan (HKH) region are largely unknown. Only on the Tibetan Plateau a long tradition of
15 permafrost research, predominantly on rather gentle relief, exists. Two permafrost maps are
16 available digitally that cover the HKH and provide estimates of permafrost extent, i.e. the
17 areal proportion of permafrost: The manually delineated Circum-Arctic Map of Permafrost
18 and Ground Ice Conditions (Brown et al., 1998) and the Global Permafrost Zonation Index,
19 based on a computer model (Gruber, 2012). This article provides a first-order assessment of
20 these permafrost maps in the HKH region based on the mapping of rock glaciers.

21 Rock glaciers were used as a proxy, because they are visual indicators of permafrost, can
22 occur near the lowermost regional occurrence of permafrost in mountains, and because they
23 can be delineated based on high-resolution remote sensing imagery freely available on
24 Google Earth. For the mapping, 4,000 square samples (approx. 30 km²) were randomly
25 distributed over the HKH region. Every sample was investigated and rock glaciers were
26 mapped by two independent researchers following precise mapping instructions. Samples
27 with insufficient image quality were recorded but not mapped.

28 We use the mapping of rock glaciers in Google Earth as first-order evidence for permafrost in
29 mountain areas with severely limited ground truth. The minimum elevation of rock glaciers
30 varies between 3,500 and 5,500 m a.s.l. within the region. The Circum-Arctic Map of
31 Permafrost and Ground Ice Conditions does not reproduce mapped conditions in the HKH

32 region adequately, whereas the Global Permafrost Zonation Index does so with more
33 success. Based on this study, the Permafrost Zonation Index is inferred to be a reasonable
34 first-order prediction of permafrost in the HKH. In the central part of the region a considerable
35 deviation exists that needs further investigations.

36 **1 Introduction**

37 Permafrost underlies much of the Earth's surface and interacts with climate, ecosystems and
38 human systems. The interaction between permafrost, or its thaw, and human activity is
39 diverse and varies with environmental and societal conditions. Examples include ground
40 subsidence, vegetation change on pasture, slope instability, hydrological change, damage to
41 infrastructure, and special requirements for construction. This list is not exhaustive and it is
42 likely that climate change will bring about unexpected permafrost phenomena and societal
43 impacts in the future (cf. Gruber, 2012, IPCC, 2014). A large proportion of the global
44 permafrost region is situated in mountain terrain. This includes densely populated areas
45 especially in the European Alps and Asian high-mountain ranges. While permafrost in
46 European mountains and its associated climate change impacts are comparably well
47 investigated, little is known about permafrost in many Asian mountain ranges. In this study,
48 we focus on the Hindu Kush Himalayan (HKH) region, which we use as one way for
49 delineating a study region in the mountains of South and Central Asia (Fig 1). The HKH
50 region includes mountains in parts of Afghanistan, Bhutan, China, India, Myanmar, Nepal
51 and Pakistan (Fig 1). Comprised mostly of high-elevation rugged terrain, including the
52 Tibetan Plateau, the Hindu Kush, Karakoram and Himalayan mountain ranges, more than
53 half of its 4.5 million km² are located above 3,500 m a.s.l. As the source of the ten largest
54 Asian river systems, the HKH region provides water, ecosystem services and the basis for
55 livelihoods to an estimated population of more than 210 million people in the mountains and
56 1.3 billion people when including downstream areas (Bajracharya and Shrestha, 2011).
57 While glaciers and glacier change have received considerable research attention in recent
58 years (e.g., Bolch et al., 2012), large areas of permafrost in the HKH region have barely or
59 only partially been investigated. The Tibetan Plateau, as the only part of the HKH region, has
60 a long tradition of permafrost research (Cheng and Wu, 2007; Yang et al., 2010; Zhang,
61 2005), most of these studies, however, focus on a narrow engineering corridor and/or on
62 rather gentle relief. Ran et al. (2012) provide an overview and comparison of the several
63 Chinese permafrost maps that include the Tibet Plateau and that reflect several decades of
64 research and development in this area. For locations with mountainous topography only
65 sporadic information exists, especially along the southern flanks of the Himalayas (Owen and
66 England, 1998, Shroder et al., 2000, Ishikawa et al., 2001, Fukui et al., 2007a, Regmi, 2008).

67 Only two permafrost maps are available digitally that cover the HKH region and provide
68 estimates of permafrost extent, i.e. the areal extend of permafrost:

69 (A) The Circum-Arctic Map of Permafrost and Ground Ice Conditions (cf. Heginbottom
70 et al., 1993, Brown et al., 1998) published by the International Permafrost Association
71 (IPA map). It is based on manually delineated polygons of classes (continuous,
72 discontinuous, sporadic, isolated patches) of permafrost extent (Heginbottom, 2002).
73 The map has been digitized and is available digitally from the Frozen Ground Data
74 Center at the National Snow and Ice Data Center (NSIDC), Boulder, Colorado, USA.

75 (B) The Global Permafrost Zonation Index (PZI), available on a spatial grid of about 1
76 km resolution (Gruber, 2012). PZI is an index representing broad spatial patterns but
77 it does not provide actual permafrost extent or probability of permafrost at a location.
78 It is based on a mathematical formulation of permafrost extent as a function of mean
79 annual air temperature, a 1 km digital elevation model and global climate data. The
80 parameterization is based on rules similar to those employed for the IPA map.
81 Additionally, the uncertainty range is explored (a) with three parameter sets
82 describing a best guess as well as conservative and anti-conservative estimates of
83 permafrost extent, and (b) using spatial fields of air temperature derived from global
84 climate reanalysis (NCAR-NCEP) and from interpolated station measurements (CRU
85 TS 2.0). Uncertainty is expressed in the resulting map product with a ‘fringe of
86 uncertainty’, referring to a permafrost extent greater than 10% in the coldest of the
87 diverse simulations performed.

88 The application of either map in the mountainous parts of the HKH region is not
89 straightforward, because (a) little information on mountainous permafrost exists to establish
90 their credibility, (b) the range of environmental conditions in the HKH region is large and
91 subject to conditions (such as monsoonal summer precipitation, hyperaridity or extreme
92 elevation) for which only limited knowledge exists, and (c) only few remote, high elevation
93 meteorological stations exist, usually in valley floors, making the application of gridded
94 climate data or the estimation of conditions in remote high-elevation areas error-prone. The
95 required testing or calibration of models (maps) of permafrost extent, unfortunately, is difficult
96 and often avoided (Gruber, 2012), both for lack of data and for lack of methods for comparing
97 point observations such as boreholes with spatial estimates of permafrost extent.

98 This study provides a first-order assessment of these two permafrost maps in the
99 mountainous part of the HKH region. We use the qualifier “first-order” as only direct
100 observation of permafrost can provide a reliable evaluation. In the absence of reliable
101 information on permafrost in this region, such a first-order assessment is useful as it adds

102 relevant information on the approximate areas of permafrost occurrence. We use rock
103 glaciers as a proxy, because they are visual indicators of permafrost, they can exist near the
104 lowermost regional occurrence of permafrost in mountains (Haeberli et al., 2006), and
105 because they can be delineated based on high-resolution remote sensing imagery freely
106 available on Google Earth. Our objectives are to (a) develop a rock glacier mapping
107 procedure that is suitable for application on Google Earth, (b) map rock glaciers in randomly
108 distributed square samples over the entire HKH region and perform quality control on the
109 resulting data, and (c) based on the mapped rock glaciers assess available permafrost
110 distribution maps.

111 **2 Background**

112 The term rock glacier is used to describe a creeping mass of ice-rich debris on mountain
113 slopes (e.g. Capps, 1910; Haeberli, 1985). The presence of ground ice at depth, usually
114 inferred from signs of recent movement, is indicative of permafrost. In areas with a
115 continental climate, commonly found in the HKH region, surface ice interacts with permafrost
116 and results in complex mixtures of buried snow or glacier ice and segregated ice formed in
117 the ground. In such environments all transitions from debris covered polythermal or cold
118 glaciers to ice cored moraines and deep-seated creep of perennially frozen sediments occur
119 (e.g. Owen and England, 1998, Shroder et al., 2000, Haeberli et al., 2006).

120 The occurrence of rock glaciers is governed not only by the ground thermal regime but also
121 by the availability of subsurface ice derived from snow avalanches, glaciers, or ice formation
122 within the ground. Furthermore, sufficient supply of debris and topography steep enough to
123 promote significant movement are required. Therefore, the presence of intact rock glaciers
124 can be used as an indicator of permafrost occurrence, but the absence of intact rock glaciers
125 does not indicate the absence of permafrost. As intact rock glaciers contain ice (latent heat)
126 and move downslope, their termini can be surrounded by permafrost-free ground. The
127 frequently occurring cover of coarse clasts promotes relatively low ground temperatures and
128 thereby further retards the melting of the ice within the rock glacier. In steep terrain, this
129 makes termini of rock glaciers local-scale indicators for the presence of permafrost,
130 sometimes occurring at an elevation indicative of the lowermost regional occurrence of
131 permafrost in mountains (Haeberli et al., 2006). This tendency of being among the lowermost
132 occurrences of permafrost in an area is exploited in this mapping exercise. In more gentle
133 terrain, such as parts of the Tibetan Plateau, not the ground thermal conditions (i.e. the
134 presence of permafrost), but the slope angle is the limiting factor. As a consequence, rock

135 glaciers can be absent over large areas of permafrost due to the lack of debris, low slope
136 angles, lack of avalanche snow or the elevation of the valley floor.

137 The spatially heterogeneous ground thermal regime and the frequent existence of
138 permafrost-free areas directly adjacent to rock glaciers makes the concept of “lower
139 permafrost limits” impractical as these limits are neither measurable nor clearly defined and
140 consequently we avoid this concept despite its prevalence in the literature. As an example,
141 the data and statistical analyses presented by Boeckli et al. (2012) show that mean annual
142 ground temperature can vary by 10–15°C locally, i.e. while subject to the same mean annual
143 air temperature. In this varied pattern of ground temperatures, rock glaciers often are among
144 the lowest regional occurrences of permafrost, given sufficient moisture supply and
145 topography. At elevations lower than the lowest rock glaciers in a region, very little
146 permafrost is to be expected whereas the proportion (extent) of permafrost usually increases
147 towards higher elevations.

148 Rock glaciers are a widespread feature in many parts of the HKH region, but very limited
149 research has been conducted on them. For the northern regions of India and Pakistan, in the
150 Karakorum Range, lowermost elevations of active rock glaciers vary between 3,850 and
151 5,100 m a.s.l. Inactive rock glaciers were even recorded at lower elevations with a minimum
152 elevation of 3,350 m a.s.l. in the Western Karakorum Range (Hewitt, 2014). A significant
153 increase in the number of rock glaciers is seen from monsoon-influenced regions in the east
154 to the dry westerly influenced regions with annual precipitation being below 1,000 mm (Owen
155 and England, 1998). From the Khumbu region in Nepal lowermost occurrences of active rock
156 glaciers are reported to be between 5,000 and 5,300 m a.s.l. (Jakob, 1992). Further east in
157 the Kangchenjunga Himal of Nepal, the distribution of rock glaciers varies from 4,800 m a.s.l.
158 on northern aspect to 5,300 m a.s.l. on south- to east-facing slopes (Ishikawa et al., 2001).
159 So far no studies have been conducted using rock glaciers as indicators for the presence of
160 permafrost on the northern side of the Himalaya. Further north, the extremely dry and cold
161 conditions on the Tibetan Plateau have resulted in a variety of permafrost related features for
162 which no occurrences in other mountain ranges are described (Harris et al., 1998).

163 For remote sensing based derivation of glacier outlines over large areas often ASTER and
164 Landsat TM have been used. Data from higher resolution sensors have rarely been applied
165 over larger areas due to costs and availability (e.g. Paul et al., 2013). With ASTER and
166 Landsat TM images at resolution of 15 m and coarser, automated mapping of rock glaciers
167 proved to be very challenging (Janke, 2001, Brenning, 2009). On a local scale rock glaciers
168 have been successfully mapped using aerial photography in the Chilean Andes (Brenning,
169 2005) the Russian Altai mountains (Fukui et al., 2007b) in Norway (Lilleøren and Etzelmüller,

170 2011) and in Iceland (Lilleøren et al., 2013). The release of freely available high-resolution
171 satellite images (i.e. Google Earth), which approach the quality of aerial photographs,
172 opened up new possibilities. The images used in Google Earth are SPOT Images or
173 products from DigitalGlobe (e.g. Ikonos, QuickBird), and they are georectified with a digital
174 elevation model (DEM) based on the Shuttle Radar Topography Mission (SRTM) data, which
175 has a 90 m resolution in the research area. In mountain regions horizontal inaccuracy for the
176 SRTM DEM can be of the same order, as Bolch et al. (2008) reported from the Khumbu
177 region in Nepal.

178 **3 Methods**

179 Inferring approximate patterns of permafrost occurrence from rock glacier mapping requires
180 four major steps: (a) identification of rock glaciers, and their status (intact vs. relict), (b)
181 mapping of the rock glaciers (c) regional aggregation to obtain a minimum elevation, and (d)
182 a method to identify the potential candidate area in which rock glaciers can be expected
183 based on topography and other environmental conditions. These four steps are described in
184 the following subchapters.

185 **3.1 Identification of rock glaciers and their status**

186 They were visually identified based on their flow patterns and structure. These included
187 transversal flow structures (ridges and furrows), longitudinal flow structures, frontal
188 appearance, and the texture difference of the rock glacier surfaces compared to the
189 surrounding slopes. The most likely origin of the ice was not used as an exclusion criterion,
190 thus also features containing glacier derived ice were considered as rock glaciers The state
191 of rock glaciers was estimated based on the visibility of a front with the appearance of fresh
192 material exposed as well as an overall convex and full shape.

193 These rules were formulated in guidelines containing example images. The mapping was
194 guided by the recording of attributes (Table 1). The recording of these attributes supported a
195 structured evaluation of each landform identified as a rock glacier and provided subjective
196 confidence scores.

197 **3.2 Mapping of rock glaciers**

198 The samples to map rock glaciers in Google Earth were created in the free statistical
199 software R (R Core Team, 2014). Each sample consists of one square polygon with a
200 specified latitudinal width [°]. The following approximate adjustment for the longitudinal width
201 [°] has been applied, where LAT [°] is the latitude for the specific sample.

$$longitudinal\ width = \frac{latitudinal\ width}{\cos\left(\frac{\pi * LAT}{180}\right)} \quad (1)$$

202 To achieve a random distribution, the investigation area was tessellated with potential
203 sample polygons, from which a predefined number of polygons were randomly selected
204 using the R-function *sample*. Every sample received a unique name consisting of two capital
205 letters and three numbers. With the R-function *kmlPolygons* from the *maptools* package
206 (Bivand and Lewin-Koh, 2013) samples were exported into a Keyhole Markup Language
207 (kml) file, which is the main data format supported by Google Earth.

208 Google Earth is frequently used to display scientific results (e.g. Scambos et al., 2007,
209 Gruber, 2012), but in some cases also as a data source (e.g. Sato & Harp, 2009). Neither
210 spectral nor spatial properties of the displayed satellite images are easily accessible. Thus
211 the accuracy of the used remote sensing images and any created output is hard to quantify.
212 Potere (2008) showed that the horizontal accuracy of 186 points in 46 Asian cities has a
213 mean root mean square error (RMSE) of 44 m when comparing them to Landsat GeoCover.
214 The accuracy of Google Earth is sufficient for our purposes as the inaccuracy thus arising
215 from horizontal misalignment between imagery and DEM is likely to be smaller than 100 m
216 vertical.

217 We mapped 4,000 samples within the HKH region. Each sample consists of one square
218 polygon with a latitudinal width of 0.05 decimal degrees equivalent to 5.53 km. Due to the
219 imperfect latitude correction of width, the area per sample varies from 26.1 km² in the south
220 to 32.2 km² in the north.

221 Manually mapped outlines of debris covered glaciers based on high-resolution images vary
222 significantly, even if mapped by experts (Paul et al., 2013). Due to similar visual properties,
223 the same kind of issues can be expected when mapping rock glaciers. To reduce
224 subjectivity, every sample was mapped by two persons independently. This was done by
225 three people with expertise based on their field of study (two holding a MSc in Glaciology and
226 one holding a MSc in Environmental Science with a focus on periglacial processes) and after
227 two months of specific training. Each sample was mapped by two different persons, resulting
228 in two comprehensive mappings. Mapping guidelines were iteratively updated and improved
229 and the final version of the guidelines was applied consistently to all samples. Regular
230 meetings were held to resolve difficulties in the mapping.

231 **3.3 Regional aggregation**

232 The elevation characteristics of the mapped rock glaciers were extracted from SRTM DEM
233 version 4.1 from CGIAR at a spatial resolution of 90 m (Jarvis et al., 2008) using ArcGIS 10.
234 For the analysis only the mapped rock glacier area within the sample polygons were taken
235 into account. Afterwards, extreme values (i.e. lowest and highest elevations of rock glacier
236 snouts) were revisited and checked, ensuring plausible results from both mappings. Even
237 though both mappings showed plausible and similar results, for the final analysis we chose to
238 only use areas identified by both persons as rock glaciers. Thus the influence of subjectivity
239 or blunders during the mapping process was further reduced, resulting in a much more
240 conservative and firm data base.

241 **3.4 The potential candidate area**

242 For the evaluation of permafrost maps, rock glaciers outside the signatures for permafrost in
243 a map indicate false negatives: the map indicates the likely absence of permafrost, but the
244 existence of permafrost can be inferred based on mapped rock glaciers. A comparison of
245 mapped rock glaciers with predicted permafrost extent, however, is only informative in
246 situations where the formation and observation of rock glaciers can be expected. As part of
247 the analysis we identify the 'potential candidate area', i.e. areas, where there is a chance to
248 map rock glaciers. This is important, as the absence of mapped rock glaciers from flat areas,
249 from glaciers, or in areas with insufficient image quality is to be expected. The potential
250 candidate area includes only sample areas, which fulfil all of the following three criteria: (a)
251 Topography: The standard deviation of the SRTM 90m DEM within the sample polygon is
252 larger 85 m. This threshold was chosen so as to be smaller than the lowest observed value
253 where rock glaciers were mapped, which is 89.5 m (b) Image quality: Only samples with
254 sufficient image quality are taken into account. (c) Absence of glaciers: Glacier covered
255 areas were excluded based on the glacier inventory published by Bajracharya and Shrestha
256 (2011), which largely covers the HKH region with the exception of parts of China.

257 **4 Results and Discussion**

258 **4.1 Data and data quality**

259 Of the 4,000 samples 3,432 (86%) received the same classification by both mapping
260 persons: 70% did not have any rock glaciers, 12% had insufficient quality and 4% contained
261 rock glaciers (Fig 3). Those 4% translate into 155 samples with 702 rock glaciers in total. In
262 3% of all samples only one mapping contained rock glaciers but the other did not.

263 The spatial distribution of classified samples shows that nearly all mapped rock glaciers are
264 located within the Himalayan arc (Fig 3). Only very few samples on the Tibetan Plateau
265 contained rock glaciers. Also, the samples with insufficient quality of the Google Earth
266 images show distinct patterns, concentrated along the Himalayan arc and eastern part of the
267 Tibetan Plateau. However, as the reasons for insufficient image qualities were not noted
268 down, no exact statements can be made. Impressions from the involved analysts were that in
269 the Himalayan arc this was mainly due to snow cover and on the Eastern Tibetan Plateau
270 mainly due to very coarse image resolutions. Clouds were only an issue in a few cases.

271 The high resolution of Google Earth images and the rigorous exclusion of samples with poor
272 image quality made it possible to discriminate rock glaciers from other (similar) landforms. It
273 was possible to assess visually the steepness or activity of the rock glacier front and the
274 characteristic of transversal and longitudinal flow structures, providing a subjectively
275 acceptable, but here not objectively testable, level of confidence in interpreting landforms as
276 indicators for the presence of permafrost. Vegetation coverage on a rock glacier was only
277 identified in two sample polygons in the whole HKH region and is either absent in the
278 investigation area, or not visible based on the imagery available. In European mountains,
279 vegetation cover has often been taken as an indication of relict rock glaciers (Cannone and
280 Gerdol, 2003) but this concept is difficult to generalize to other mountain ranges. The two
281 cases mapped here have been disregarded for further analysis.

282 On the scale of one sample polygon, the mapped outlines of rock glaciers varied
283 considerably between the two mappings by the analysts. Major differences occurred
284 especially in the somewhat arbitrary delineation of the upper boundary of rock glaciers and
285 the separation between individual objects, whereas a higher congruence existed for the
286 termini of mapped rock glaciers (Fig 4). This resulted in relatively small differences when
287 comparing the mean minimum elevation of all mapped rock glaciers per sample from the two
288 mappings. The mean difference between the two mappings is 46 m (Fig 4). Samples with
289 high differences were mostly a result of a different number of mapped rock glaciers.

290 The differences in sample size with changing latitude are not expected to influence the
291 results for the minimum elevation of rock glaciers per sample. A slight error biased towards a
292 higher minimum elevation for rock glaciers can be expected due to rock glaciers which are
293 only partially within the mapped sample. In those cases their lowest point has been taken at
294 the sample boarder and not at the rock glacier snout. With respect to the comparably large
295 data base, neither inaccuracies originating from Google Earth nor from the SRTM DEM
296 should distort the further products.

297 This estimation of data quality can be put into perspective by comparison with findings from
298 other mountain ranges and by comparing with expected maximum uncertainty in the
299 permafrost maps to be evaluated. In the European Alps, a difference of about 2°C (Table 2 of
300 Boeckli et al 2012) in mean annual air temperature has been found between intact and relict
301 rock glaciers, providing an order of magnitude for possible errors induced by
302 misinterpretation of rock glacier status. Gruber (2012) uses well-established approximations
303 of permafrost occurrence based on mean annual air temperature to estimate permafrost
304 occurrence. At the same time, that publication shows differences of more than 4°C in long-
305 term mean annual air temperature between differing gridded data products. Given that this is
306 likely a conservative estimate of the true error in these data products and considering the
307 spatially diverse lapse rates (e.g., Kattel et al. 2013), our uncertainty in pinpointing zones
308 with permafrost in the mountainous HKH is likely to be much larger than 6°C, or about 600–
309 1000 m in elevation. Even with the uncertainty due to imperfect identification of rock glaciers
310 and their activity status, systematic mapping of rock glaciers can reduce this uncertainty – or
311 point to differences between the mapping and simulations based on air temperature fields
312 where additional research is needed. Furthermore, the documentation of visible signs of
313 permafrost throughout the region is important in supporting the growing realization that
314 permafrost really does occur in these mountains.

315 **4.2 Regional rock glacier distribution**

316 Minimum elevations reached by rock glaciers are expressed as a mean on the sample scale
317 (approx. 30 km²), taking into account the lowermost points of all mapped rock glaciers and
318 thus resulting in a mean minimum elevation per sample. This provides a more robust and
319 conservative measure than a minimum value, but also implies that some rock glaciers do
320 reach lower elevations than indicated by the sample mean value. Mean minimum elevations
321 reached by rock glaciers per sample vary significantly in the HKH region (Fig 5). They are a
322 few hundred meters lower than what previous more local studies have reported for Nepal
323 (Jakob, 1992, Ishikawa et al., 2001) and match well with previous reports from Pakistan
324 (Owen and England, 1998).. The lowest elevation was recorded in Northern Afghanistan at
325 3,554 m a.s.l. and the highest elevation at 5,735 m a.s.l. on the Tibetan Plateau. If variations
326 within close proximity occur, they follow regional patterns. The most pronounced shift of the
327 mean minimum elevation reached by rock glaciers occurs between the southern and the
328 northern side of the Himalaya, where the mean minimum elevation rises several hundred
329 meters within a short distance.

330 **4.3 Assessment of permafrost distribution maps**

331 Fig 6 and Fig 7 show how the termini of the mapped rock glaciers relate to the signatures of
332 the maps evaluated. The mapped rock glaciers are distributed evenly over all classes of the
333 PZI (Fig 6). Rock glacier density per class peaks for the medium PZI values and decreases
334 towards both ends of the spectrum. The decrease is more pronounced towards lower PZI
335 values (lower possibility of permafrost). Only 5 out of more than 700 mapped rock glaciers
336 are reaching areas outside the PZI. Thus the PZI is in good agreement with our study, based
337 on this summary evaluation.

338 When comparing the mapped rock glaciers with the IPA map (Fig 7) the investigation area
339 and the mapped rock glaciers are predominantly in the two classes Discontinuous
340 Permafrost and Sporadic Permafrost. A small part of the investigation area and a few
341 mapped rock glaciers are in the class Isolated Permafrost. The class Continuous Permafrost
342 does not exist in the HKH region. More than 250 of the mapped rock glaciers are outside the
343 IPA map permafrost signature. Thus the IPA map does not coincide well with the findings
344 from our study. This is likely due to simplification and subjectivity in the applied manual
345 mapping, but in part may stem from inaccuracies in the digitization and coordinate
346 transformation of the map into the digital product available from NSIDC.

347 **4.4 Regional comparison with the Permafrost Zonation Index**

348 Spatial patterns of the agreement between the PZI and the mapped rock glaciers are shown
349 in Fig 8 aggregated to 1° x 1° resolution. Mapped rock glaciers are reaching low PZI values
350 in most parts of the investigation area and thus indicate a good agreement. Only for the
351 northern side of the central part of the Himalayan arc the lowest elevation of mapped rock
352 glacier remains in high PZI values, despite the presence of low PZI values, thus showing that
353 the minimum elevation reached by rock glaciers and the predicted lowermost occurrence of
354 permafrost are not in agreement. Therefore, either the PZI (due to its method or its driving
355 data) fails to reproduce the local permafrost conditions or the conditions for rock glacier
356 development in the particular area are different from other areas of the region. This may
357 partially be caused by the topography of the Tibetan Plateau, where the lower elevations,
358 and thus lower PZI values, correspond with a flatter topography. Further, there are very
359 distinctive climatic conditions in this region, with a strong south-north precipitation gradient
360 due to the Himalaya blocking the summer monsoon on the southern slopes, resulting in
361 extremely dry and continental conditions on the Tibetan Plateau. Consequently, we assume
362 that rock glaciers may not reach the predicted lowermost occurrence of permafrost as they

363 may not form because of sparse supply of snow to be incorporated in aggrading debris. But
364 to test this hypothesis further, more detailed investigations are needed.

365 **5 Conclusions**

366 Comparison of the two rock glacier mappings showed relatively small differences, as
367 described in Section 4.1, indicating that the proposed mapping procedure works consistently.
368 By using only the intersected area from two independent mappings, subjectivity as described
369 for the manual delineation of debris covered glaciers by Paul et al. (2013) could further be
370 reduced. Thus the use of Google Earth as a data source to map rock glaciers in a data
371 sparse region is shown to be feasible.

372 The diversity of the climate in the investigation area leads to a wide morphological range of
373 rock glaciers, or features of apparently moving debris, exceeding what is commonly
374 observed in Europe and North America. Over the whole investigation area, the minimum
375 elevation of rock glaciers varies from 3,500 m a.s.l. in Northern Afghanistan to more than
376 5,500 m a.s.l. on the Tibetan Plateau. A clear increase in the minimum elevation reached by
377 rock glaciers can be observed towards the Tibetan Plateau.

378 There are two permafrost distribution maps available for the HKH region, the IPA map with
379 manually delineated permafrost classes (Brown et al., 1998) and the PZI which is based on a
380 simple computer model (Gruber, 2012). Comparing these two maps with the mapped rock
381 glaciers from our study is a first step in assessing their quality for the remote and data sparse
382 mountainous parts of the HKH region. The IPA map falls short in adequately representing
383 local permafrost conditions with more than 250 of the mapped rock glaciers falling outside its
384 permafrost signature. The PZI map and the rock glacier mapping on the other hand are in
385 good agreement, with only 5 mapped rock glaciers being outside the PZI. Based on the
386 information available, PZI does indicate areas where no permafrost can be expected rather
387 well and is currently the best prediction of the permafrost distribution in the HKH region.

388 In most areas, the lowermost mapped rock glaciers coincide with low PZI values. There is,
389 however, a disagreement in the central part of the region, where rock glaciers do not reach
390 down to elevations with low PZI values. This disagreement can inform further research and it
391 underscores the importance of using the presence of rock glaciers as an indicator of
392 permafrost but to not use their absence as an indicator of permafrost free conditions. The
393 comparison with the rock glacier mapping is a first step towards more thorough testing of the
394 PZI, and other models and map products for this remote and data sparse region.

395

396 **Author contribution**

397 M.O.S. developed the method; conducted the analysis and prepared the manuscript. S.G.
398 conceived the study, supervised the development of the method and the analysis, and
399 contributed significantly to the writing. P.B, S.S. and T.S. did the mapping and provided
400 general support. D.S. and P.W. contributed to conceiving the study, secured funding,
401 provided overall supervision and contributed to the writing.

402 **Data availability**

403 The rock glaciers mapping, the source code to create the random samples and the outline of
404 the HKH region is published as supplementary material. Both mappings include all 4,000
405 samples and all mapped rock glaciers. Different colours indicate the different persons
406 involved in the mapping. Those files come in KML (Keyhole Markup Language) and can be
407 opened with Google Earth and most GIS software. The file f.RandomPolygon.r contains the
408 R-function to create the samples.

409 **Acknowledgments**

410 This study was supported by ICIMOD through core funding by the Department for
411 International Development (DFID) of the United Kingdom and by the governments of
412 Afghanistan, Australia, Austria, Bangladesh, Bhutan, China, India, Myanmar, Nepal, Norway,
413 Pakistan, and Switzerland. The views and interpretations in this publication are those of the
414 authors. They are not necessarily attributable to ICIMOD and do not imply the expression of
415 any opinion by ICIMOD concerning the legal status of any country, territory, city or area of its
416 authority, or concerning the delimitation of its frontiers or boundaries, or the endorsement of
417 any product.

418

419 **References**

- 420 Bajracharya, S. and Shrestha, B.: The status of glaciers in the Hindu Kush-Himalayan
421 region., ICIMOD, Kathmandu., 2011.
- 422 Bivand, R. and Lewin-Koh, N.: mapproj: Tools for reading and handling spatial objects,
423 [online] Available from: <http://cran.r-project.org/package=mapproj>, 2013.
- 424 Boeckli, L., Brenning, A., Gruber, S. & Noetzli, J. 2012. A statistical approach to modelling
425 permafrost distribution in the European Alps or similar mountain ranges, *The Cryosphere*, 6:
426 125–140, doi:10.5194/tc-6-125-2012, 2012.
- 427 Bolch, T., Buchroithner, M., Pieczonka, T. and Kunert, A.: Planimetric and volumetric glacier
428 changes in the Khumbu Himal, Nepal, since 1962 using Corona, Landsat TM and ASTER
429 data, *J. Glaciol.*, 54(187), 592–600, doi:10.3189/002214308786570782, 2008.
- 430 Bolch, T., Kulkarni, A., Käab, A., Huggel, C., Paul, F., Cogley, J. G., Frey, H., Kargel, J. S.,
431 Fujita, K., Scheel, M., Bajracharya, S. and Stoffel, M.: The state and fate of Himalayan
432 glaciers., *Science*, 336(6079), 310–4, doi:10.1126/science.1215828, 2012.
- 433 Brenning, A.: Geomorphological, hydrological and climatic significance of rock glaciers in the
434 Andes of Central Chile (33–35°S), *Permafr. Periglac. Process.*, 16(3), 231–240,
435 doi:10.1002/ppp.528, 2005.
- 436 Brenning, A.: Benchmarking classifiers to optimally integrate terrain analysis and
437 multispectral remote sensing in automatic rock glacier detection, *Remote Sens. Environ.*,
438 113(1), 239–247, doi:10.1016/j.rse.2008.09.005, 2009.
- 439 Brown, J., Ferrians, O., Heginbottom, J. A. and Melnikov, E.: *Circum-Arctic Map of*
440 *Permafrost and Ground-Ice Conditions.*, Boulder, Color. USA Natl. Snow Ice Data Center.,
441 1998.
- 442 Cannone, N. and Gerdol, R.: Vegetation as an Ecological Indicator of Surface Instability in
443 Rock Glaciers, Arctic, Antarct. Alp. Res., 35(3), 384–390, doi:10.1657/1523-
444 0430(2003)035[0384:VAAEIO]2.0.CO;2, 2003.
- 445 Capps, S. R.: Rock Glaciers in Alaska, *J. Geol.*, 18(4), 359–375, 1910.
- 446 Cheng, G. and Wu, T.: Responses of permafrost to climate change and their environmental
447 significance, Qinghai-Tibet Plateau, *J. Geophys. Res.*, 112(F2), F02S03,
448 doi:10.1029/2006JF000631, 2007.
- 449 Cremonese, E., Gruber, S., Phillips, M., Pogliotti, P., Boeckli, L., Noetzli, J., Suter, C., Bodin,
450 X., Crepaz, A., Kellerer-Pirklbauer, A., Lang, K., Letey, S., Mair, V., Morra di Cella, U.,
451 Ravanel, L., Scapozza, C., Seppi, R. & Zischg, A.: Brief Communication: “An inventory of
452 permafrost evidence for the European Alps.” *The Cryosphere* 5: 651–657, doi:10.5194/tc-5-
453 651-2011, 2011.
- 454 Fukui, K., Fujii, Y., Ageta, Y. and Asahi, K.: Changes in the lower limit of mountain
455 permafrost between 1973 and 2004 in the Khumbu Himal, the Nepal Himalayas, *Glob.*
456 *Planet. Change*, 55(4), 251–256, doi:10.1016/j.gloplacha.2006.06.002, 2007a.

- 457 Fukui, K., Fujii, Y., Mikhailov, N., Ostanin, O. and Iwahana, G.: The lower limit of mountain
458 permafrost in the Russian Altai Mountains, *Permafr. Periglac. Process.*, 18(2), 129–136,
459 doi:10.1002/ppp.585, 2007b.
- 460 Gruber, S.: Derivation and analysis of a high-resolution estimate of global permafrost
461 zonation, *Cryosph.*, 6(1), 221–233, doi:10.5194/tc-6-221-2012, 2012.
- 462 Haeberli, W.: Creep of mountain permafrost: internal structure and flow of alpine rock
463 glaciers, *Mitteilungen der Versuchsanstalt für Wasserbau, Hydrol. und Glaziologie an der*
464 *ETH Zurich*, (77), 5–142, 1985.
- 465 Haeberli, W., Hallet, B., Arenson, L., Elconin, R., Humlum, O. and Ka, A.: Permafrost Creep
466 and Rock Glacier Dynamics, *Permafr. Periglac. Process.*, 17, 189–214, doi:10.1002/ppp,
467 2006.
- 468 Harris, S. a., Zhijiu, C. and Guodong, C.: Origin of a bouldery diamicton, Kunlun Pass,
469 Qinghai-Xizang Plateau, People's Republic of China: gelifluction deposit or rock glacier?,
470 *Earth Surf. Process. Landforms*, 23(10), 943–952, doi:10.1002/(SICI)1096-
471 9837(199810)23:10<943::AID-ESP913>3.0.CO;2-7, 1998.
- 472 Heginbottom, J. A.: Permafrost mapping: a review, *Prog. Phys. Geogr.*, 26(4), 623–642,
473 doi:10.1191/0309133302pp355ra, 2002.
- 474 Heginbottom, J. A., Brown, J., Melnikov, E. S. and O.J. Ferrians, J.: Circum-arctic map of
475 permafrost and ground ice conditions, *Proc. Sixth Int. Conf. Permafrost*, 5–9
476 July, 1993, Beijing, China, 255–260, 1993.
- 477 Hewitt, K.: *Glaciers of the Karakoram Himalaya*, Springer Netherlands, Dordrecht., 2014.
- 478 IPCC: Summary for Policymakers. In: *Climate Change 2014: Impacts, Adaptation, and*
479 *Vulnerability. Part A: Global and Sectoral Aspects. Contribution of Working Group II to the*
480 *Fifth Assessment Report of the Intergovernmental Panel on Climate Change* [Field, C.B.,
481 V.R. Barros, D.J. Dokken, K.J. Mach, M.D. Mastrandrea, T.E. Bilir, M. Chatterjee, K.L. Ebi,
482 Y.O. Estrada, R.C. Genova, B. Girma, E.S. Kissel, A.N. Levy, S. MacCracken, P.R.
483 Mastrandrea, and L.L. White (eds.)]. Cambridge University Press, Cambridge, United
484 Kingdom and New York, NY, USA, pp. 1-32, 2014.
- 485 Ishikawa, M., Watanabe, T. and Nakamura, N.: Genetic differences of rock glaciers and the
486 discontinuous mountain permafrost zone in Kanchanjunga Himal, Eastern Nepal, *Permafr.*
487 *Periglac. Process.*, 12(3), 243–253, doi:10.1002/ppp.394, 2001.
- 488 Jakob, M.: Active rock glaciers and the lower limit of discontinuous alpine permafrost,
489 Khumbu Himalaya, Nepal, *Permafr. Periglac. Process.*, 3(April), 253–256, 1992.
- 490 Janke, J. R.: Rock Glacier Mapping: A Method Utilizing Enhanced TM Data and GIS
491 Modeling Techniques, *Geocarto Int.*, 16(3), 5–15, doi:10.1080/10106040108542199, 2001.
- 492 Jarvis, A., Reuter, H. I., Nelson, A. and Guevara, E.: Hole-filled SRTM for the globe Version
493 4, [online] Available from: <http://srtm.csi.cgiar.org>, 2008.
- 494 Jiandong, X., Bo, Z., Liuyi, Z. and Zhengquan, C.: Field geological exploration of Ashikule
495 volcano group in western Kunlun Mountains, *Earthq. Resarch China*, 26(2), 2–9, 2011.

- 496 Kattel, D.B., Yao, T., Yang, K., Tian, L., Yang, G., and Joswiak, D.: Temperature lapse rate in
497 complex mountain terrain on the southern slope of central Himalayas, *Theor. Appl.*
498 *Climatol.*, 113:671–682 doi:10.1007/s00704-012-0816-6, 2013.
- 499 Lilleøren, K. S. and Etzelmüller, B.: A regional inventory of rock glaciers and ice-cored
500 moraines in Norway, *Geogr. Ann. Ser. A, Phys. Geogr.*, 93(3), 175–191, doi:10.1111/j.1468-
501 0459.2011.00430.x, 2011.
- 502 Lilleøren, K. S., Etzelmüller, B., Gärtner-Roer, I., Kääh, A., Westermann, S. and
503 Guðmundsson, Á.: The Distribution, Thermal Characteristics and Dynamics of Permafrost in
504 Tröllaskagi, Northern Iceland, as Inferred from the Distribution of Rock Glaciers and Ice-
505 Cored Moraines, *Permafr. Periglac. Process.*, 24(4), 322–335, doi:10.1002/ppp.1792, 2013.
- 506 Owen, L. A. and England, J.: Observations on rock glaciers in the Himalayas and Karakoram
507 Mountains of northern Pakistan and India, *Geomorphology*, 26(1-3), 199–213,
508 doi:10.1016/S0169-555X(98)00059-2, 1998.
- 509 Paul, F., Barrand, N. E., Baumann, S., Berthier, E., Bolch, T., Casey, K., Frey, H., Joshi, S.
510 P., Konovalov, V., Bris, R. Le, Mölg, N., Nosenko, G., Nuth, C., Pope, A., Racoviteanu, A.,
511 Rastner, P., Raup, B., Scharrer, K., Steffen, S. and Winsvold, S.: On the accuracy of glacier
512 outlines derived from remote-sensing data, *Ann. Glaciol.*, 54(63), 171–182,
513 doi:10.3189/2013AoG63A296, 2013.
- 514 Potere, D.: Horizontal Positional Accuracy of Google Earth's High-Resolution Imagery
515 Archive, *Sensors*, 8(12), 7973–7981, doi:10.3390/s8127973, 2008.
- 516 R Core Team: R: A Language and Environment for Statistical Computing, [online] Available
517 from: <http://www.r-project.org/>, 2014.
- 518 Ran, Y., Li, X., Cheng, G., Zhang, T., Wu, Q., Jin, H. and Jin, R.: Distribution of Permafrost in
519 China: An Overview of Existing Permafrost Maps, *Permafr. Periglac. Process.*, 23(4), 322–
520 333, doi:10.1002/ppp.1756, 2012.
- 521 Regmi, D.: Rock Glacier distribution and the lower limit of discontinuous mountain permafrost
522 in the Nepal Himalaya, *Proc. Ninth Int. Conf. Permafr. (NICOP)*, June 29–July 3, 2008,
523 Alaska Fairbanks, 1475–1480, 2008.
- 524 Sato, H. P. and Harp, E. L.: Interpretation of earthquake-induced landslides triggered by the
525 12 May 2008, M7.9 Wenchuan earthquake in the Beichuan area, Sichuan Province, China
526 using satellite imagery and Google Earth, *Landslides*, 6(2), 153–159, doi:10.1007/s10346-
527 009-0147-6, 2009.
- 528 Scambos, T., Haran, T., Fahnestock, M. A., Painter, T. H. and Bohlander, J.: MODIS-based
529 Mosaic of Antarctica (MOA) data sets: Continent-wide surface morphology and snow grain
530 size, *Remote Sens. Environ.*, 111(2-3), 242–257, doi:10.1016/j.rse.2006.12.020, 2007.
- 531 Shroder, J. F., Bishop, M. P., Copland, L. and Sloan, V. F.: Debris-covered Glaciers and
532 Rock Glaciers in the Nanga Parbat Himalaya, Pakistan, *Geogr. Ann. Ser. A Phys. Geogr.*,
533 82(1), 17–31, doi:10.1111/j.0435-3676.2000.00108.x, 2000.

534 Yang, M., Nelson, F. E., Shiklomanov, N. I., Guo, D. and Wan, G.: Permafrost degradation
535 and its environmental effects on the Tibetan Plateau: A review of recent research, *Earth-*
536 *Science Rev.*, 103(1-2), 31–44, doi:10.1016/j.earscirev.2010.07.002, 2010.

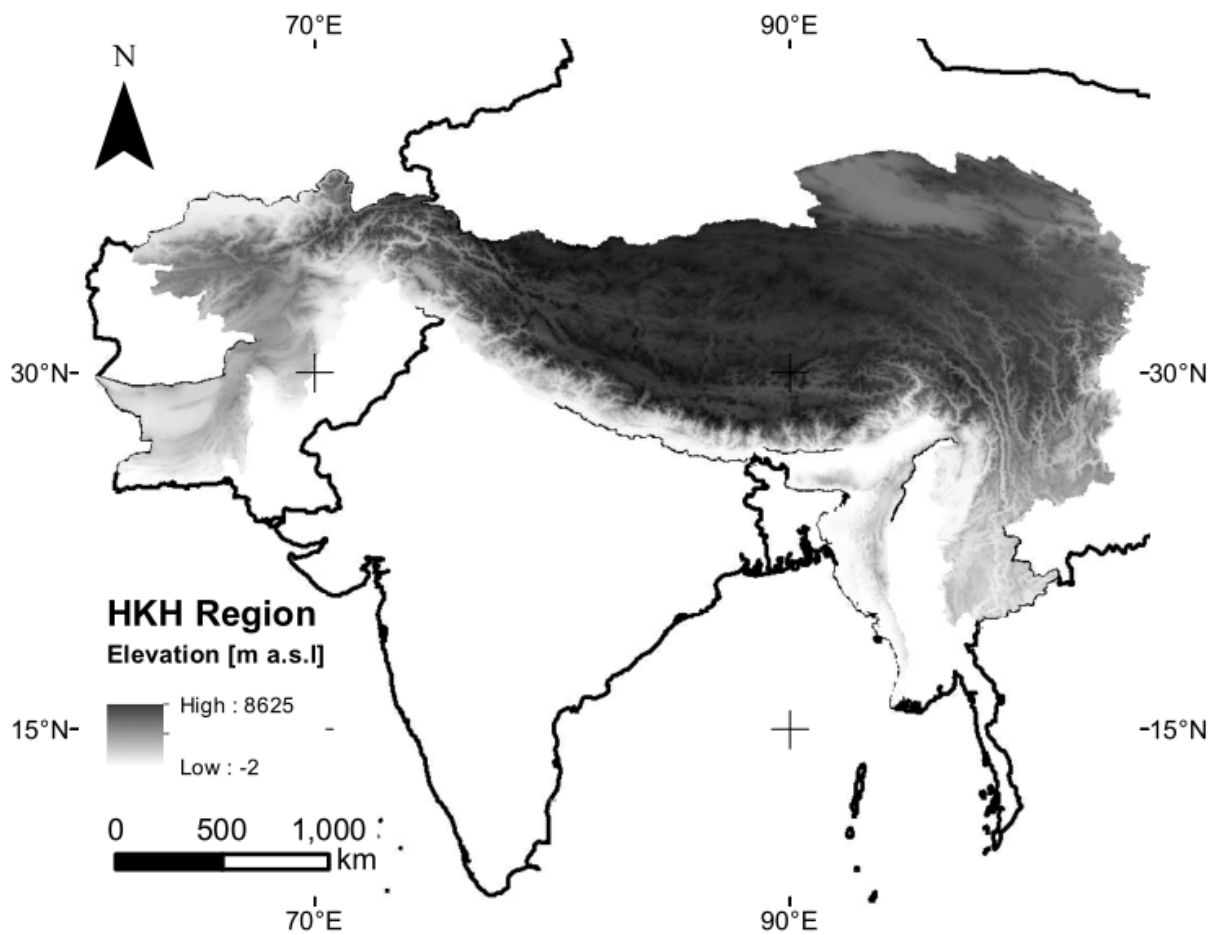
537 Zhang, T.: Historical Overview of Permafrost Studies in China, *Phys. Geogr.*, 26(4), 279–
538 298, doi:10.2747/0272-3646.26.4.279, 2005.

539

540 **Table 1: Attributes derived during rock-glacier mapping. They are recorded in the**
 541 ***Description* field of each rock glacier outline as described in the supplement to this**
 542 **publication.**

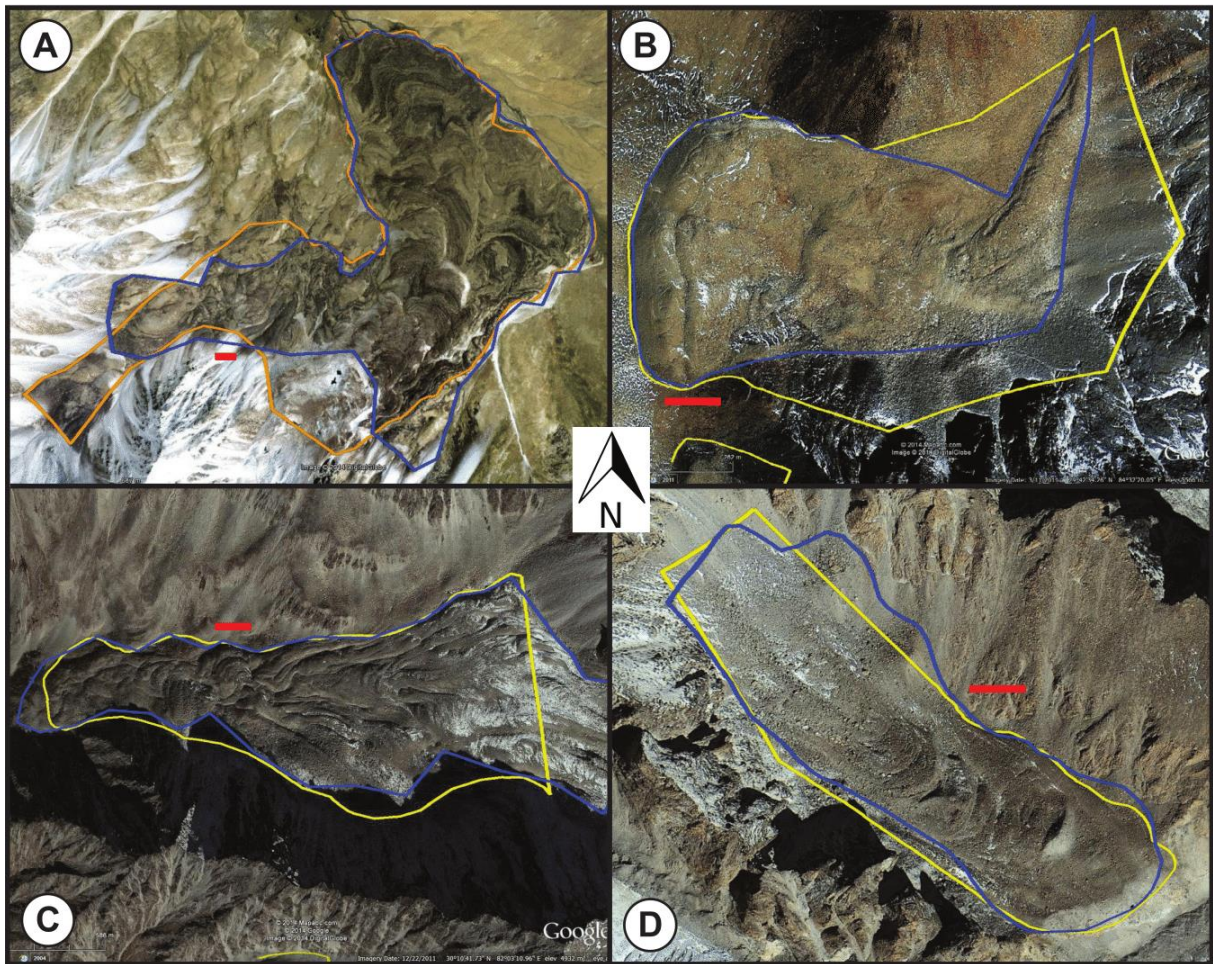
Attributes	Classification	Code
Image date	MMDDYYYY	
Upslope Boundary	Glacial	BG
	Slope	BS
	Unclear	BU
Likelihood active	Virtually Certain	AVC
	High	AH
	Medium	AM
Longitudinal Flow Structure	Clear	LC
	Vague	LV
	None	LN
Transversal Flow Structure	Clear	TC
	Vague	TV
	None	TN
Front	Steep	FS
	Gentle	FG
	Unclear	FU
Outline	Clear	OC
	Fair	OF
	Vague	OV
Snow coverage	Snow	SS
	Partial Snow	SP
	No Snow	SN
Overall Confidence	Virtually Certain	CVC
	High	CH
	Medium	CM

543



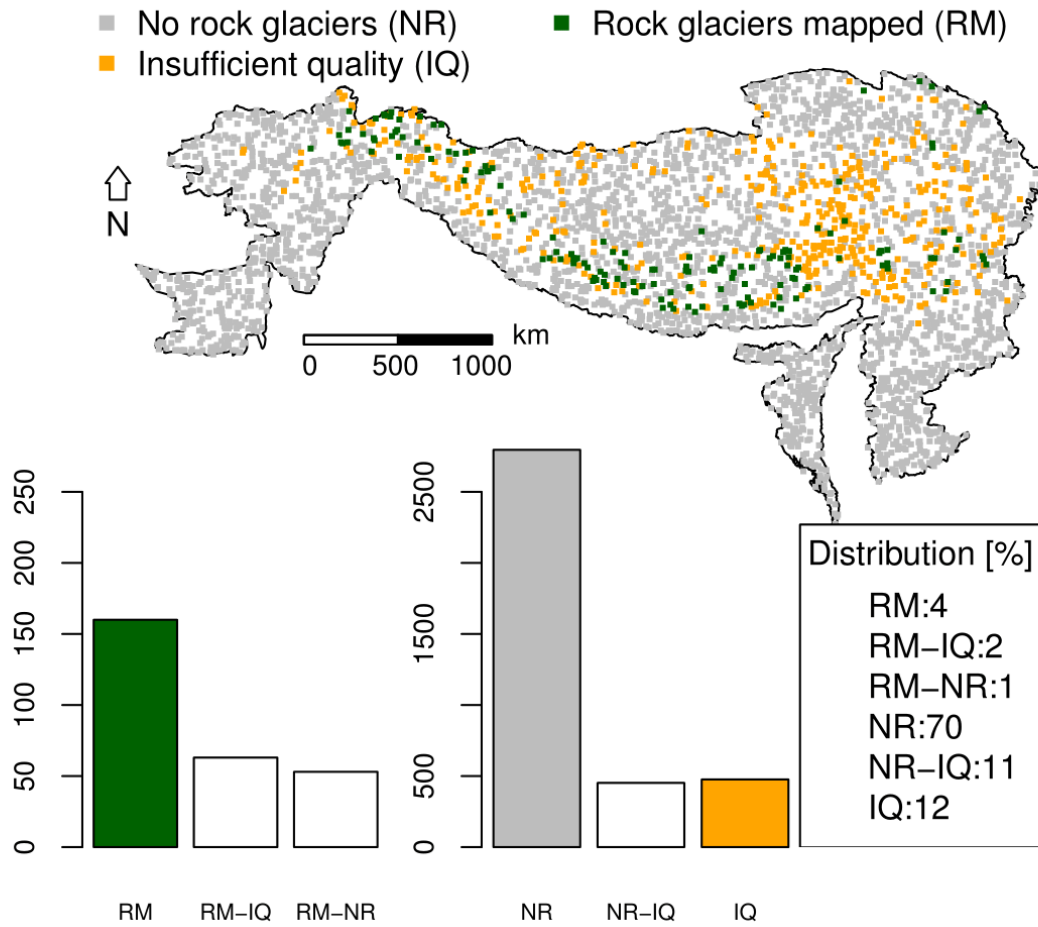
544

545 **Fig 1: The HKH region as defined by ICIMOD which includes high mountains in**
 546 **Afghanistan, Bhutan, China, India, Myanmar, Nepal and Pakistan. SRTM DEM version**
 547 **4.1 from CGIAR at a spatial resolution of 90 m (Jarvis et al., 2008) shown in the WGS84**
 548 **coordinate system.**



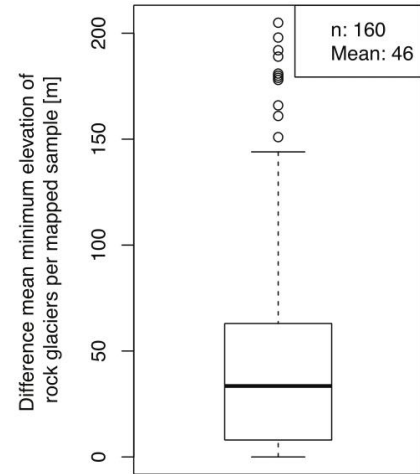
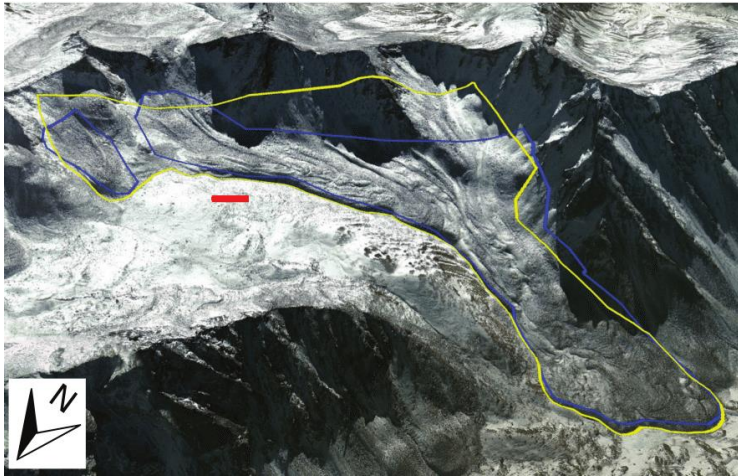
549

550 **Fig 2: Examples of rock glaciers mapped by two different persons (red line = 100m).**
 551 **Coordinates (Lat / Lon) are for A: 37.07 / 72.92; B: 29.71 / 84.54; C: 30.18 / 82.05; D:**
 552 **30.18 / 82.22. All copyrights Image © 2014 DigitalGlobe.**



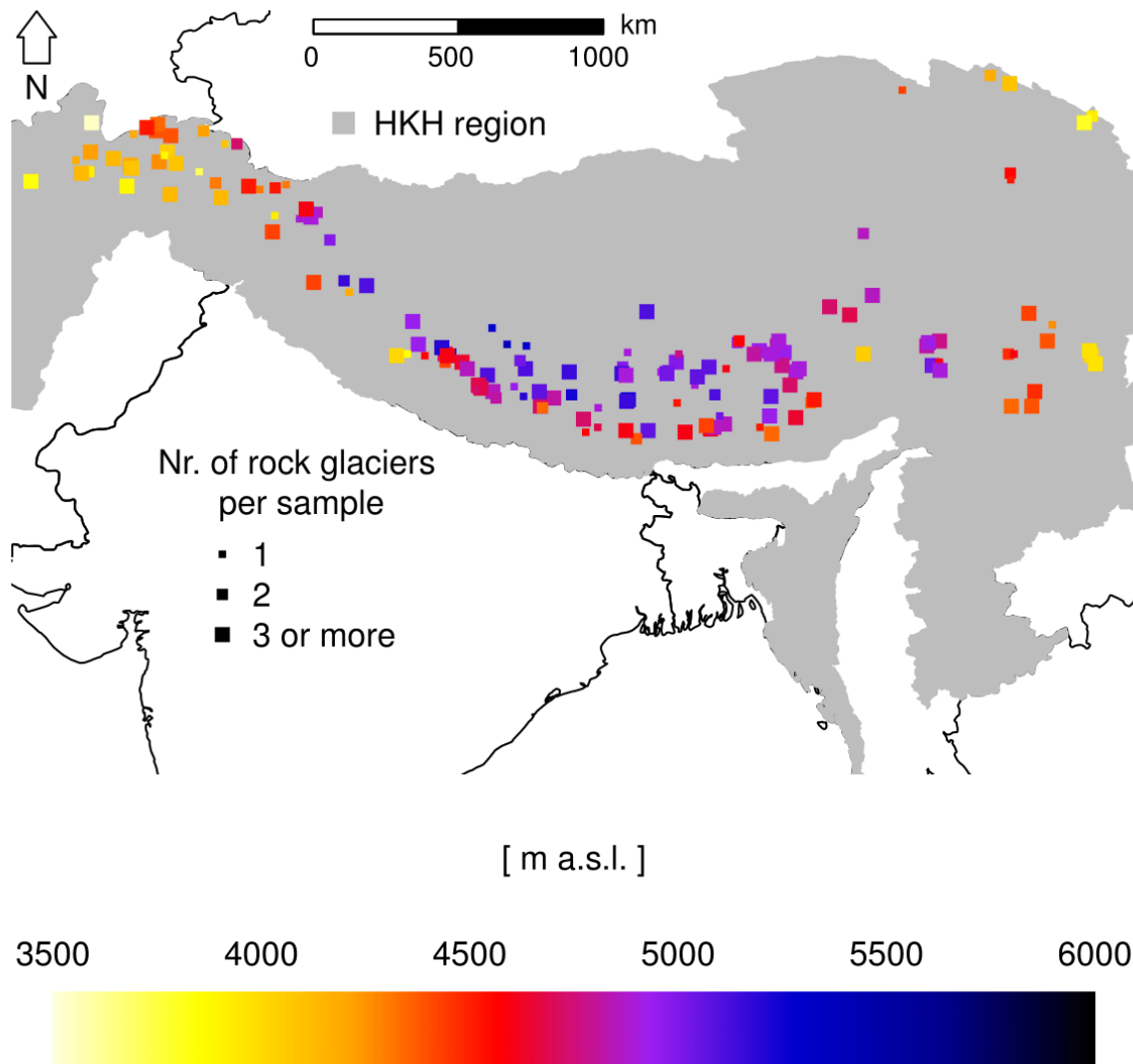
553

554 **Fig 3: Overview of mapping results. All 3,432 samples with the same classification**
 555 **from both mappings are shown. In the barplots, identically classified samples are**
 556 **shown with filled bars and samples, which were classified differently in white. Bars**
 557 **with only one abbreviation (e.g. RM) mean that both mapping persons had the same**
 558 **classification of the sample (e.g. rock glacier mapped), whereas two abbreviations**
 559 **(e.g. RM-IQ) mean that the mappings resulted not in the same classification (once rock**
 560 **glacier mapped, once insufficient quality). Note that the difference in scale between**
 561 **the samples containing rock glaciers on the left and all others samples on the right is**
 562 **one order of magnitude.**



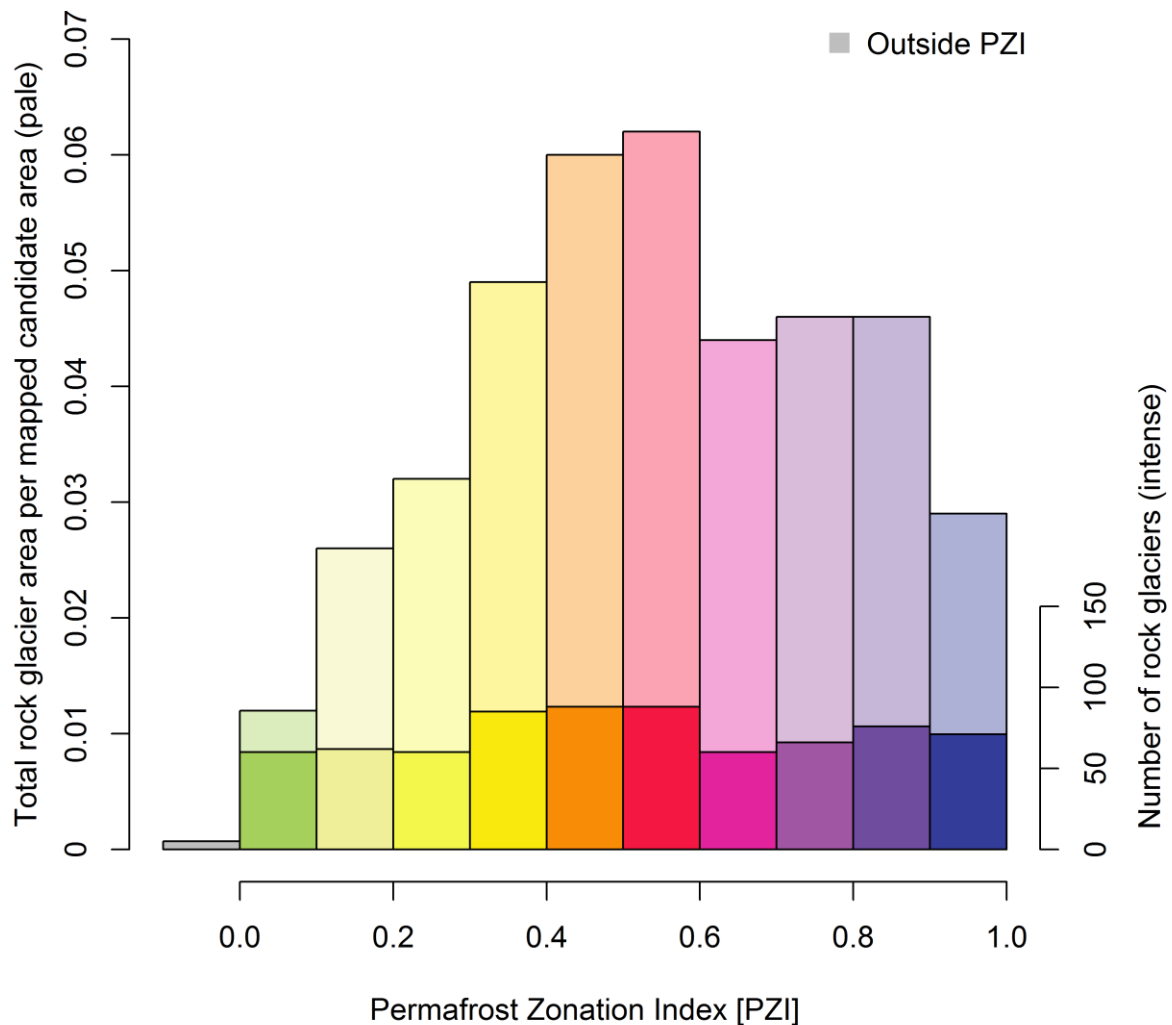
563

564 **Fig 4: Example of differences between two mappings on the left (red line = 100m).**
 565 **Copyright Image © 2014 DigitalGlobe. For the boxplot on the right only samples where**
 566 **both analysts have mapped rock glaciers were taken into account. The samples with**
 567 **big differences typically have only few rock glaciers, therefore if one object got**
 568 **mapped by only one analyst the mean minimum elevation could change significantly.**



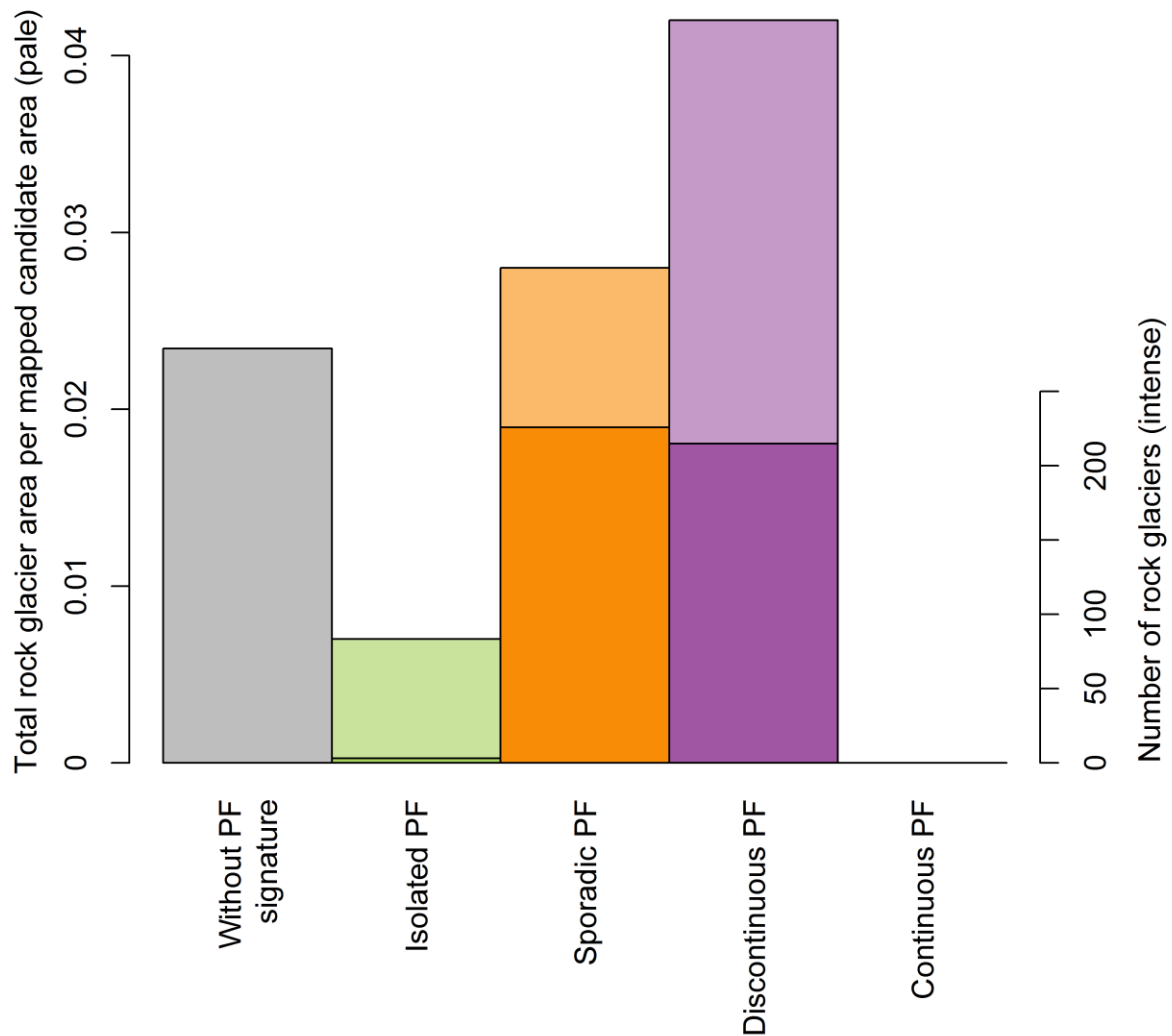
569

570 **Fig 5: Mean minimum elevation of rock glaciers per sample. The size of the square**
 571 **indicates how many rock glaciers this value is based on. This is for 24% one rock**
 572 **glacier, for 18% two rock glaciers and for 58% between three and 21 rock glaciers.**



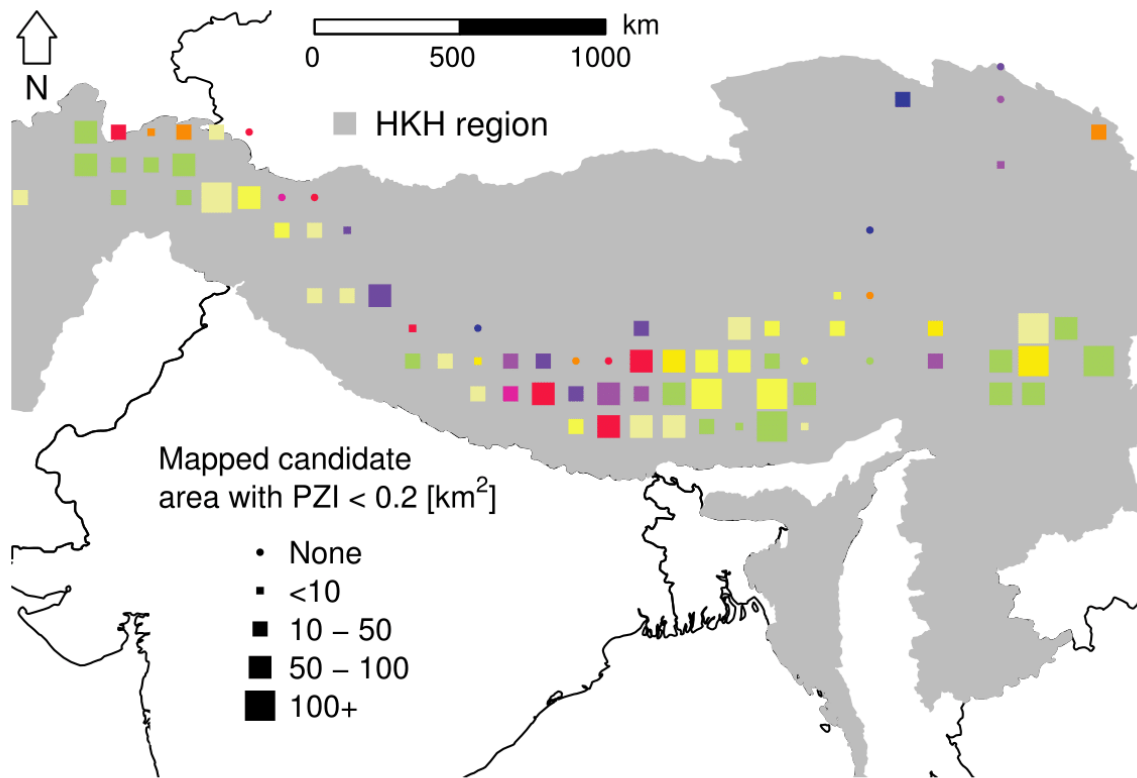
573

574 **Fig 6: Mapped rock glaciers in relation to Permafrost Zonation Index summarized over**
 575 **the mapped HKH region. Mapped candidate area refers to areas in where rock glaciers**
 576 **can be expected to occur and to be observed; for each pixel, this is determined based**
 577 **on (a) topography (standard deviation of SRTM90 > 85m in each sample), (b) sufficient**
 578 **image quality in Google Earth, and (c) the absence of glacier cover. The same colours**
 579 **as for the PZI map have been used where dark blue indicates permafrost in nearly all**
 580 **conditions and bright yellow indicates permafrost only in very favourable conditions.**
 581 **Green indicates the fringe of uncertainty. Intensive colours indicate the number of**
 582 **rock glaciers and pale colours represent the density of rock glaciers within a certain**
 583 **class. For more information on the PZI see Gruber (2012).**



584

585 **Fig 7: Comparison of all mapped rock glaciers with the Circum-Arctic Map of**
 586 **Permafrost (IPA map). Note that the category Continuous Permafrost does not occur**
 587 **in the investigation area. Mapped candidate area refers to areas in where rock glaciers**
 588 **can be expected to occur and to be observed; for each pixel, this is determined based**
 589 **on (a) topography (standard deviation of SRTM90 > 85m in each sample), (b) sufficient**
 590 **image quality in Google Earth, and (c) the absence of glacier cover. Intensive colours**
 591 **indicate the number of rock glaciers and pale colours represent the density of rock**
 592 **glaciers within a certain class.**



Legend of Permafrost Zonation Index (PZI) map used



593

594 **Fig 8: Spatial patterns of agreement between mapped rock glaciers and PZI. Colour**
 595 **indicates the lowest PZI value in the mapped rock glaciers within each 1° x 1° square.**
 596 **Green and yellow are signalling an apparent good agreement between lowest**
 597 **elevations reached by rock glaciers and predicted lowest possible elevations for**
 598 **permafrost by the PZI. The size of square symbols indicates the size of the mapped**
 599 **candidate area with PZI < 0.2. This is a proxy for whether or not rock glaciers with low**
 600 **PZI values can be expected in this area.**